original article

Resident dendritic cells are the predominant TNF-secreting cell in early renal ischemia–reperfusion injury

X Dong[1,2], S Swaminathan[1,2], LA Bachman[1], AJ Croatt[1], KA Nath[1] and MD Griffin[1]

[1]Division of Nephrology and Hypertension, Department of Medicine, Mayo Clinic College of Medicine, Rochester, Minnesota, USA

Renal ischemia–reperfusion injury (IRI) rapidly induces production of inflammatory mediators including, and in particular, tumor necrosis factor (TNF). Possible sources include resident parenchymal and bone marrow-derived cells as well as recruited leukocytes. Cell suspensions from kidneys subjected to IRI were examined by cell separation followed by in vitro culture and enzyme-linked immunosorbent assay (ELISA), immunoperoxidase and immunofluorescence microscopy, and multicolor flow cytometry to determine the contribution of dendritic cells (DCs) to early production of TNF and other inflammatory mediators. Secretion of TNF, interleukin (IL-6), monocyte chemoattractant protein-1 (MCP-1), and regulated on activation normal T cell expressed and secreted (RANTES) was increased in cell suspensions from IRI compared with control kidneys and was higher in DC-enriched preparations. Immunostaining identified TNF^{+ve} cells that coexpressed the DC marker CD11c. Flow cytometry of bone marrow-derived (CD45^{+ve}) cell populations at 24 h post-IRI demonstrated that F4/80^{+ve}/CD11c^{+ve} DCs remained proportionately stable and exhibit higher levels of DC maturation markers, whereas the proportion of F4/80^{-ve} DCs, monocytes, neutrophils, and T cells increased. Intracellular staining for TNF confirmed that F4/80^{+ve} DCs were the predominant TNF^{+ve} cell and expressed higher levels than other TNF^{+ve} cells. In vivo depletion of DCs from the kidney substantially attenuated TNF secretion by total and CD45^{+ve} cells following IRI. The results uncover a role for resident F4/80^{+ve} DCs as the predominant secretors of TNF within 24 h of IRI.

Correspondence: MD Griffin, Mayo Clinic, 200 First St SW, Rochester, Minnesota 55905, USA. E-mail: griffin.matthew@mayo.edu

[2]These authors contributed equally to this work

A critical role for inflammation in the pathophysiology of acute ischemia–reperfusion injury (IRI) of the kidney is currently well accepted on the basis of experimental and clinical studies carried out over the past two decades.[1–3] A number of proinflammatory cytokines and chemokines have been consistently implicated in the pathophysiology of acute renal failure among the most prominent of which is tumor necrosis factor (TNF). Upregulation of mRNA and protein levels of TNF occurs at a whole-organ level within minutes to hours of onset of IRI and other forms of acute renal parenchymal injury.[4–7] Less well appreciated at present is the degree to which individual cell populations contribute to the early production of TNF and other proinflammatory cytokines and chemokines within the renal interstitial compartment.[8] Although marginated and infiltrating cell populations, once recruited, likely secrete such products, the timing of the initial secretory burst in multiple models, and the requirement for secreted chemokines to initiate recruitment of these cells indicates a primary role for resident cell populations. Renal tubular epithelial cells are the predominant parenchymal cell type in the kidney and clearly can be induced to synthesize and secrete inflammatory mediators in vitro or in vivo.[9,10] The primary importance of epithelial cell-derived products, however, has not been established. Other resident cell types that may participate in the early inflammatory response to acute renal injury include endothelial cells, fibroblasts, mesangial cells, tissue macrophages, and dendritic cells (DCs).

Although least well studied among these cell types, DCs may be uniquely involved in the pathogenesis of acute renal injury for numerous reasons. DCs are known to be abundantly present throughout the renal interstitial space and directly interposed between the tubular epithelium and the peritubular capillaries in the healthy kidney.[11–13] Additionally, we and others have demonstrated that renal DCs (rDCs) undergo dynamic phenotypic alterations in the context of acute systemic or localized renal parenchymal injury.[14–19] Moreover, in keeping with the well-recognized role of DCs in initiating cognate immunity, rDC responses to such insults may include antigen uptake, migration to draining lymph nodes, and increased capacity for localized antigen-specific T-cell activation – functional activities which

occur within 2–7 days of an injurious event.[15,17] In this study, we have examined the contribution of rDCs to the early release of innate (proinflammatory) immune mediators within the acutely ischemic kidney in the mouse. Focusing predominantly on TNF production, the results identify rDCs, specifically F4/80-expressing rDCs, as potent 'first responders' in the innate response to renal IRI.

RESULTS

CD11c^{+ve} cells are potent early producers of proinflammatory mediators in the kidney following IRI

Unilateral renal artery clipping was employed to examine the contribution of intrarenal DCs to the production of proinflammatory cytokines and chemokines following IRI. Cell suspensions of clipped and unclipped kidneys, prepared 24 h after unilateral IRI, were divided into total, CD11c-enriched, and CD11c-depleted fractions using anti-CD11c microbeads and magnetic column separation (see Figure 1a) and were tested *in vitro* for secretion of TNF, interleukin (IL-6), monocyte chemoattractant protein-1 (MCP-1), and regulated on activation normal T cell expressed and secreted (RANTES) by enzyme-linked immunosorbent assay (ELISA) of culture supernatants. Secretion of these products by equal numbers of CD11c-enriched and CD11c-depleted cells was compared (Figure 1b). As shown, secretion of all four products was enhanced in culture supernatants from clipped compared to unclipped kidneys, and was markedly greater in the CD11c-enriched compared to CD11c-depleted fractions. The contribution of CD11c^{+ve} cells to overall secretion of the same products was examined by comparing concentrations in culture supernatants from unfractionated cells to those from equal numbers of CD11c-depleted cells (Figure 1c). For all products measured, depletion of CD11c^{+ve} cells from the ischemic kidney preparations was associated with reduced concentration. In this, and multiple similar experiments, the effect of CD11c depletion was most marked for TNF and RANTES compared with MCP-1 and IL-6. The increased secretion of proinflammatory products by CD11c-enriched fractions following IRI was reproduced in two other inbred mouse strains BALB/C and the lipopolysaccharide (LPS)-resistant strain C3H/HeJ, data not shown).

To more specifically visualize TNF^{+ve} cells within kidney cell suspensions, and to colocalize TNF and CD11c expression, cell preparations from clipped and control kidneys were examined by immunoperoxidase staining with anti-TNF and by three-color immunofluorescent staining with anti-TNF, anti-CD11c, and 4′,6-diamidino-2-phenylindole (DAPI) (Figure 2). Compared to control kidneys, cell preparations from IRI kidneys contained numerically greater numbers of TNF^{+ve} cells that were predominantly small and rounded (Figure 2a and b). Immunofluorescence microscopy confirmed the presence of TNF and CD11c double-positive cells within cell preparations from IRI kidneys (Figure 2c). This series of experiments was interpreted, as indicating that CD11c^{+ve} cells, presumably DCs, constitute potent inducible
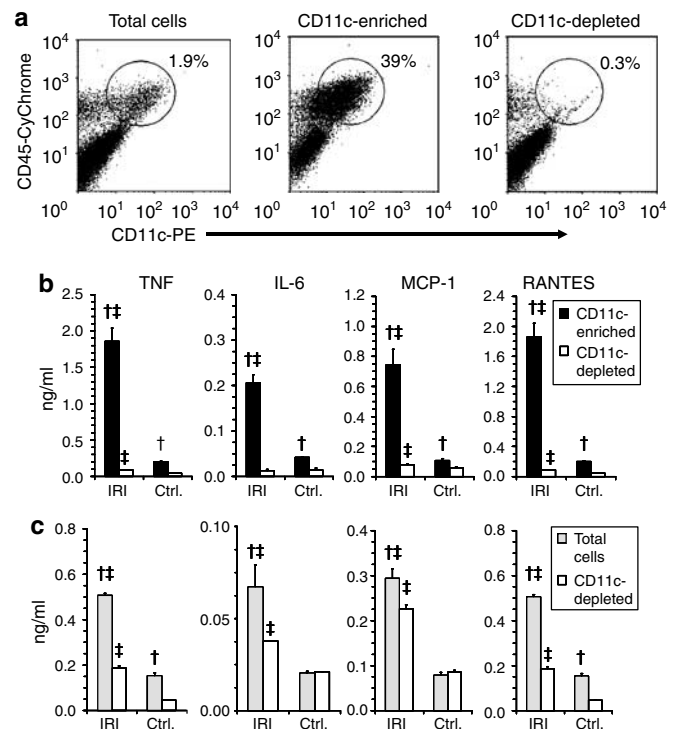
Figure 1 | CD11c^{+ve} cells are a potent source of TNF, IL-6, MCP-1, and RANTES in kidney cell suspensions following IRI. (a) Examples of flow cytometric analysis of total kidney cell suspensions and of CD11c-enriched and CD11c-depleted fractions prepared by anti-CD11c magnetic column separation. Proportions of each cell population stained positively for CD45 and CD11c are indicated. (b) Cell suspensions from clipped (IRI) kidneys and unclipped (Ctrl.) kidneys of a group of four mice were prepared 24 h after being subjected to 30 min of unilateral renal artery clipping. The cells were separated into CD11c-enriched and CD11c-depleted fractions, and were cultured overnight in equal numbers. Results are shown for ELISAs of culture supernatants from the cell fractions expressed as mean ± s.d. concentration in ng/ml. Concentrations of all four products were higher in supernatants from CD11c-enriched fractions, and were increased in CD11c-enriched cells from IRI compared to Ctrl kidneys. (c) Unsorted and CD11c-depleted cell fractions from the same organs were cultured overnight in equal numbers. Results are shown for ELISAs of culture supernatants from the cell fractions expressed as mean ± s.d. concentration in ng/ml. For IRI kidneys, concentrations of all four products were higher in supernatants from unsorted compared with CD11c-depleted fractions. For control kidneys, only TNF and RANTES were higher in unsorted fractions. Levels of all products were higher in all fractions from IRI compared with the equivalent fraction of Ctrl kidneys. † = $P<0.05$ for CD11c-enriched vs CD11c-depleted (b) or total cells vs CD11c-depleted (c). ‡ = $P<0.05$ for IRI vs Ctrl kidneys.

secretors of TNF and other proinflammatory mediators within 24 h of IRI.

CD11c^{+ve} DCs are resident intrarenal cells that are distinct from infiltrating monocytes, neutrophils, and T cells and undergo maturation *in situ* following IRI

To more definitively distinguish rDCs from other intrarenal cell populations and to further characterize TNF^{+ve} DCs during IRI, flow cytometric analysis was undertaken. Characterization of CD45^{+ve}/CD11c^{+ve} cells from healthy mouse kidneys revealed that, consistent with DCs, they were
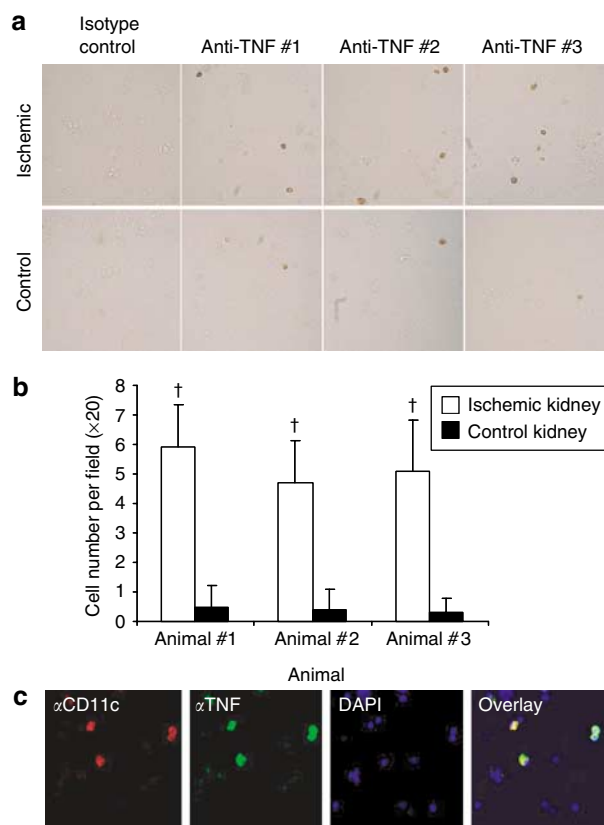
Figure 2 | Direct identification of CD11c^{+ve}, TNF-expressing cells in immunostained cell preparations from ischemic kidneys.
(**a**) Cell suspensions of ischemic and control kidneys from three adult mice were prepared 24 h following a 30 min unilateral renal artery clipping, were cultured on coverslips in the presence of a Golgi-export inhibitor, then fixed and stained by immunoperoxidase method with anti-TNF or isotype control antibody, and examined by light microscopy for positively stained cells. Isotype control staining yielded no positive staining. Small, rounded, positively stained cells were readily detected among anti-TNF stained cells of ischemic kidneys. Similar positively stained cells were detected rarely among anti-TNF stained cells of control kidneys. (**b**) Graphical representation of cell counts per high-power field are expressed for each pair of ischemic and control kidneys as mean ± s.d. for cell counts from 10 individual fields for each organ. † = *P* < 0.05 for ischemic vs control kidney. (**c**) Representative example of immunofluorescence microscopy of cell preparation from an ischemic kidney following culture in the presence of a Golgi-export inhibitor and staining with anti-CD11c-PE, anti-TNF-AF488, and DAPI. Overlaid images demonstrate multiple cells staining for both CD11c and TNF.

positive for markers of professional antigen-presenting cells (MHC II, CD80, CD86, CD54 (ICAM-1), CD1d) but negative for subset markers of lymphoid organ DCs (CD8α, CD4, CD205 (DEC205), 33D1). They were also positive for CD11b and CD16/CD32 (FcRγ II/III) but negative for the tissue macrophage markers CD169 (sialoadhesin) and CD204 (scavenger receptor type A). A subset of the renal CD45^{+ve}/CD11c^{+ve} cells, however, also expressed surface F4/80 and intracellular CD68 suggesting a phenotypic overlap with macrophages (Figure S9). Cell suspensions, prepared 24 h after unilateral IRI from clipped and control kidneys, were stained for the pan-leukocyte marker CD45 in combination
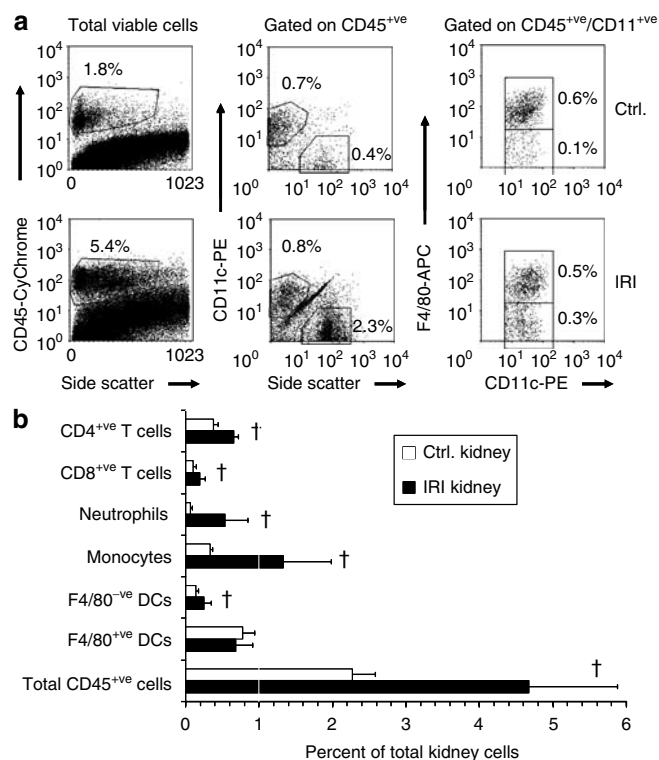

Figure 3 | Elucidation and enumeration of CD45^{+ve} cell populations in ischemic and control kidneys. Cell suspensions from kidneys of adult mice 24 h following a 30 min unilateral renal artery clipping were stained for CD45 in combination with antibodies against CD11c (DC marker), Ly6C (monocyte marker), Ly6G (neutrophil marker), and CD3ε (T-cell marker). DCs were additionally stained for F4/80. T cells were additionally stained for CD4 and CD8. (**a**) Examples of multicolor flow cytometric analyses to distinguish DCs from monocytes in cell suspensions from unclipped (Ctrl) and clipped (IRI) kidneys and to quantify total CD45^{+ve} cells (left dot plots), CD45^{+ve}/CD11c^{+ve}/Ly6C^{-ve} and CD45^{+ve}/CD11c^{-ve}/Ly6C^{+ve} cells (middle dot plots) and CD45^{+ve}/CD11c^{+ve}/F4/80^{+ve} and CD45^{+ve}/CD11c^{+ve}/F4/80^{-ve} cells (right dot plots). For cell populations of interest (boxed regions), the quantification is expressed as percentage of the total viable cells. (**b**) Results of a complete analysis of CD45^{+ve} cell populations from Ctrl and IRI kidneys of a group of four mice subjected to unilateral renal artery clipping are shown graphically and expressed as mean ± s.d. percent of the total population of kidney cells analyzed. Staining definitions for each cell populations were as follows CD4-pos T cells: CD45^{+ve}/CD11c^{-ve}/CD3ε^{+ve}/CD4^{+ve}; CD8-pos T cells: CD45^{+ve}/CD11c^{-ve}/CD3ε^{+ve}/CD8^{+ve}; neutrophils: CD45^{+ve}/CD11c^{-ve}/Ly6G^{+ve}; monocytes: CD45^{+ve}/CD11c^{-ve}/Ly6C^{+ve}; F4/80-neg DCs: CD45^{+ve}/CD11c^{+ve}/Ly6C^{-ve}/F4/80^{-ve}; and F4/80-pos DCs: CD45^{+ve}/CD11c^{+ve}/Ly6C^{-ve}/F4/80^{+ve}. All CD45^{+ve} cell populations were proportionally increased in IRI kidneys with the exception of F4/80-pos DCs, which were unchanged. † = *P* < 0.05 for IRI compared with Ctrl kidneys.

with CD11c, F4/80, and either Ly6C, Ly6G, or CD3ε (to distinguish monocytes, neutrophils, and T cells, respectively). T cells were further stained for CD4 and CD8. Examples of staining for CD45, CD11c, Ly6C, and F4/80 and of the relative quantification of positively stained subsets are shown in Figure 3a. Results of the overall analysis of CD45^{+ve} cell subsets in clipped and control kidneys from a representative experiment, expressed as percent of the total cell suspensions

at 24 h postclipping, are presented in Figure 3b. Compared to contralateral, nonischemic kidneys, IRI resulted in an increased proportion of total CD45^{+ve} cells and of monocytes (CD45^{+ve}/CD11c^{-ve}/Ly6C^{+ve}), neutrophils (CD45^{+ve}/CD11c^{-ve}/Ly6G^{+ve}), CD8 T cells (CD45^{+ve}/CD11c^{-ve}/CD3ε^{+ve}/CD8^{+ve}), CD4 T cells (CD45^{+ve}/CD11c^{-ve}/CD3ε^{+ve}/CD8^{+ve}), and F4/80^{-ve} DCs (CD45^{+ve}/CD11c^{+ve}//Ly6C^{-ve}/F4/80^{-ve}). In contrast, the proportion of F4/80^{+ve} DCs (CD45^{+ve}/CD11c^{+ve}/Ly6C^{-ve}/F4/80^{+ve}) remained unchanged. In separate experiments, higher expression levels of DC maturation markers were demonstrated for CD45^{+ve}/CD11c^{+ve}/F4/80^{+ve} cells from ischemic kidneys 24 h after renal artery clipping. As shown in Figure 4a and b, IRI was associated with relatively larger cell size (as reflected by forward scatter) and higher surface levels of MHC II, CD80, CD86, CD40, and CD54 (ICAM-1) on these cells. These data demonstrate that (a) F4/80^{+ve} DCs constitute a major proportion of the resident bone marrow-derived cells within the healthy kidney. (b) During the first 24 h following IRI, intrarenal F4/80^{+ve} DCs remain proportionately stable, whereas other leukocyte populations are proportionately increased. (c) The F4/80^{+ve} DCs within ischemic kidneys exhibit a more mature phenotype than those of nonischemic kidneys.

Resident F4/80^{+ve} DCs are the most significant cell population expressing high TNF levels following IRI

The involvement of bone marrow-derived (CD45^{+ve}) cells and the relative contributions of different CD45^{+ve} lineages in TNF production following IRI was further evaluated by surface and intracellular staining with flow cytometric analysis. As shown in Figure 5a and b, IRI resulted in a proportionate increase in TNF^{+ve} cells within total kidney cell suspensions. The large majority of the TNF^{+ve} cells from ischemic kidneys were CD45^{+ve} (Figure 5c). Additional surface staining for DCs (CD11c), monocytes (Ly6C), neutrophils (Ly6G), and T cells (CD3ε) indicated that, while DCs constituted 20–25% of all CD45^{+ve} cells from ischemic kidneys, they represented 55–60% of the CD45^{+ve}/TNF^{+ve} cells at this time point (Figure 6a). The second most numerous CD45^{+ve}/TNF^{+ve} cells were Ly6C^{+ve} monocytes representing 18–22% of the total. Neutrophils and T cells were rare among TNF^{+ve} cells. Importantly, when mean fluorescence intensity for anti-TNF staining was compared between DCs and monocytes from ischemic kidneys, the result indicated significantly higher TNF expression in DCs (Figure 6b). The specific predominance of F4/80-expressing DCs among TNF^{+ve} cells of ischemic kidneys was confirmed by CD45 enrichment of kidney cell suspensions 24 h after renal artery clipping followed by surface staining for CD11b, CD11c, and F4/80, and intracellular staining for TNF. As illustrated in Figure 7, the large majority of TNF^{+ve} cells in this cell preparation were located within a dense cluster of CD11c^{+ve}/CD11b^{+ve}/F4/80^{+ve} cells.

In a final experimental strategy, depletion of intrarenal DCs was carried out by intravenous injection of clodronate-
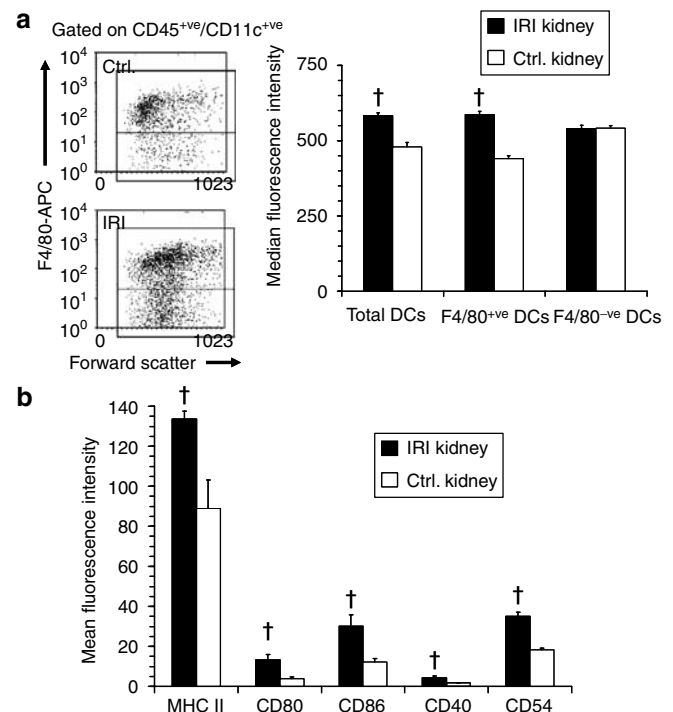

Figure 4 | Upregulation of DC maturation markers on F4/80^{+ve} DCs in kidneys following IRI. Cell suspensions from kidneys of adult mice ($n = 4$) 24 h following a 30 min unilateral renal artery clipping were stained for CD45, CD11c, and F4/80 in combination with a panel of antibodies against DC maturation markers (MHC II (I-Ab), CD80, CD86, CD54, and CD40). (**a**) Representative dot plots are shown for unclipped (Ctrl) and clipped (IRI) kidney preparations gated on CD45^{+ve}/CD11c^{+ve} cells (total DCs) and analyzed for forward scatter and anti-F4/80 staining. Gating of F4/80^{+ve} DCs and F4/80^{-ve} DCs is indicated (boxes). Graphical representation of the results for a group of four mice is shown and indicates increased forward scatter of F4/80^{+ve} (but not F4/80^{-ve}) DCs in IRI compared with Ctrl kidneys. Results are expressed as mean ± s.d. of the median fluorescence intensities. (**b**) Graphical representation of surface staining levels (mean ± s.d. of mean fluorescence intensity) for MHC II, CD80, CD86, CD54, CD40 on F4/80^{+ve}/CD11c^{+ve} DCs from the same pairs of IRI and Ctrl kidneys. † = $P < 0.05$ for IRI kidney vs Ctrl kidney.

containing liposomes before unilateral renal artery clipping. As illustrated in Figure 8a, clodronate (but not inert (phosphate-buffered saline (PBS)) liposomes resulted in discrete depletion of CD45^{+ve}/CD11c^{+ve} cells from the kidney without depletion of other CD45^{+ve} cells (including CD45^{+ve}/Ly6C^{+ve} monocytes, Figure S10). Twenty-four hours after unilateral clipping, total, CD45-enriched, and CD45-depleted cell fractions were prepared from clipped and unclipped kidneys of mice that were pretreated with clodronate-containing liposomes or PBS liposomes. Flow cytometric analysis of the cell preparations confirmed that CD45^{+ve} cells from ischemic and nonischemic kidneys of clodronate-treated animals were devoid of CD11c^{+ve} DCs but were otherwise similar in composition to those from animals treated with inert liposomes (data not shown). Secretion of TNF was compared for equal numbers of CD45-enriched and CD45-depleted cells, and for equal numbers of unfractionated and CD45-depleted cells (Figure 8b). In
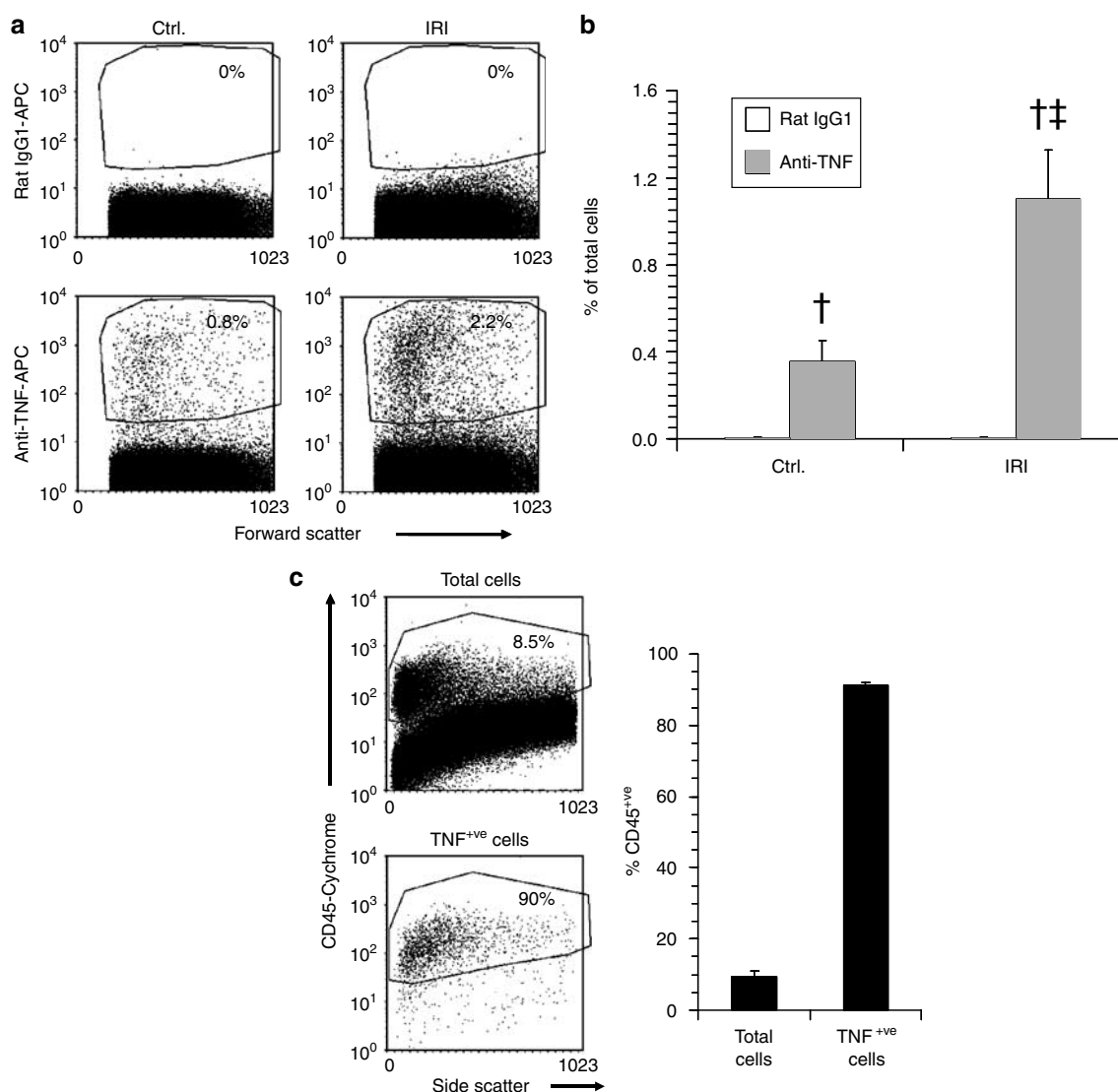
Figure 5 | TNF-expressing cells are increased in kidneys following IRI and are predominantly bone marrow derived (CD45^{+ve}). Cell suspensions were prepared from unclipped (Ctrl) and clipped (IRI) kidneys of adult mice ($n=3$) 24 h following a 30 min unilateral renal artery clipping. The cells were surface stained for CD45 and intracellularly stained with Rat IgG1-APC or anti-TNF-APC. (**a**) Representative dot plots of forward scatter vs rat IgG-APC or anti-TNF-APC fluorescence are shown for total analyzed cells from Ctrl and IRI kidney. TNF^{+ve} cells (lower dot plots) are readily distinguished and gated for further analysis. Quantification is indicated as percent of the total cells analyzed for each dot plot. (**b**) Graphical presentation of the mean ± s.d. percent of total cells stained with anti-TNF compared with rat IgG1 in Ctrl and IRI kidneys. † = $P<0.05$ for anti-TNF vs rat IgG1, ‡ = $P<0.05$ for IRI vs Ctrl. (**c**) Representative dot plots for side scatter vs anti-CD45 fluorescence are shown for total cells and for TNF^{+ve} cells from one of the four IRI kidneys from the same experiment (left panel). CD45^{+ve} cells are readily distinguished (boxes) representing 8.5% of the total cells and 90% of the TNF^{+ve} cells. Results for all four IRI kidneys are shown graphically (right panel) as mean ± s.d. of %CD45^{+ve} among total cells and TNF^{+ve} cells.

agreement with previous experiments, IRI was associated with increased TNF secretion by kidney-derived cell suspensions. Virtually all the TNF secreted was derived from CD45^{+ve} cells. In addition, however, depletion of intrarenal DCs before onset of IRI resulted in substantial reduction in the amount of TNF secreted by total kidney cells as well as by CD45^{+ve} cells on a cell-for-cell basis. This result provided confirmation that maximal intrarenal TNF production following IRI is dependent on the presence of resident DCs.

DISCUSSION

The kidney is susceptible to functional decline following systemic events such as hypotension, septicemia, or drug/toxin exposure, and following localized perturbations including those that interrupt organ blood flow or urinary outflow. The renal dysfunction associated with these diverse causes of acute renal parenchymal injury results, at least in part, from the generation and secretion of innate immune mediators as well as the coordinated recruitment and functional activation of immune cell populations from the
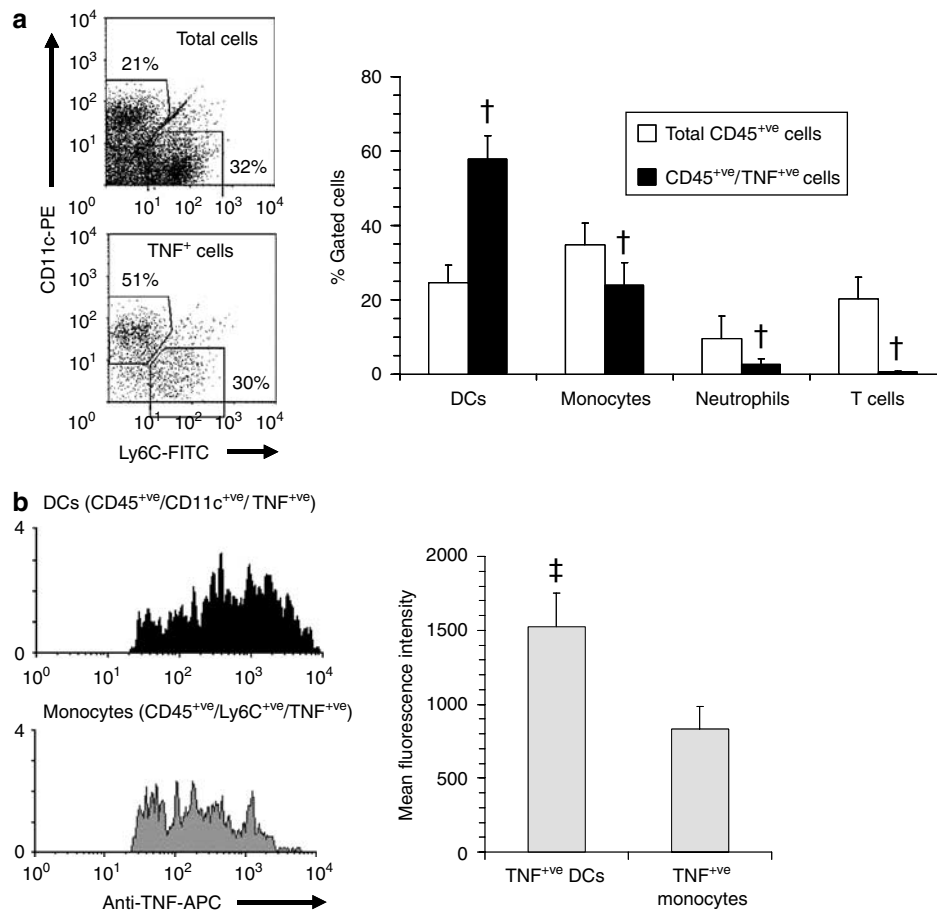
Figure 6 | DCs are the predominant high-level TNF-producer among CD45^{+ve} cell subsets in kidneys following IRI. Cell suspensions from kidneys of adult mice 24 h following a 30 min renal artery clipping were stained for CD45, CD11c, and intracellular TNF in combination with antibodies against Ly6C (monocyte marker), Ly6G (neutrophil marker), or CD3ε (T-cell marker). (a) Left panel: representative dot plots used to distinguish DCs from monocytes among total CD45^{+ve} cells and CD45^{+ve}/TNF^{+ve} are shown for one of the four IRI kidneys. The percentage of the gated cells that are CD11c^{+ve}/Ly6C^{-ve} (DCs) and CD11c^{-ve}/Ly6C^{+ve} (monocytes) are indicated. Right panel: Results of a complete analysis of the proportions of DCs, monocytes, neutrophils, and T cells among total CD45^{+ve} cells and CD45^{+ve}/TNF^{+ve} cells are shown graphically for IRI kidneys expressed as mean ± s.d. percent of the gated cells. Staining definitions for each cell populations were as follows: DCs: CD45^{+ve}/CD11c^{+ve}/Ly6C^{-ve}; monocytes: CD45^{+ve}/CD11c^{-ve}/Ly6C^{+ve}; neutrophils: CD45^{+ve}/CD11c^{-ve}/Ly6G^{+ve}; and T cells: CD45^{+ve}/CD11c^{-ve}/CD3ε^{+ve}. † = $P < 0.05$ for total CD45^{+ve} vs CD45^{+ve}/TNF^{+ve}. (b) Left panel: representative histograms are shown for fluorescence level of TNF^{+ve} DCs (CD45^{+ve}/CD11c^{+ve}/Ly6C^{-ve}/TNF^{+ve}) and monocytes (CD45^{+ve}/CD11c^{+ve}/Ly6C^{-ve}/TNF^{+ve}) from one of the four IRI kidneys. Right panel: graphical presentation of TNF expression level (mean ± s.d. of the mean fluorescence intensities) of TNF^{+ve} DCs and monocytes from four IRI kidneys. ‡ = $P < 0.05$ for TNF^{+ve} DCs vs TNF^{+ve} monocytes.

circulation.[1–3,20] Cellular sources of the proinflammatory mediators of acute renal injury are multiple and likely vary during the time course of postinjury organ dysfunction. The results of this study indicate that resident DCs are a major secretor of TNF and other proinflammatory mediators during the first 24 h following interruption of renal blood flow in this model of IRI.

Initial experiments indicated that CD11c-enriched preparations from kidney cell suspensions secreted substantially greater amounts of the cytokines TNF and IL-6, and the chemokines MCP-1 and RANTES compared with an admixture of renal cells depleted of CD11c-expressing constituents. The proportionate contribution of CD11c^{+ve} cells to overall production of these mediators (determined by comparing secretion by the total cell suspension with equal numbers of CD11c-depleted cells) was variable. In repeated

experiments carried out at 24 h post-IRI, we found that CD11c-depletion was associated with >75% reduction of TNF and RANTES, 40–60% reduction in IL-6 and 20–30% reduction of MCP-1. It should be noted that these experiments alone do not formally rule out the presence of additional rare cell types capable of producing high levels of one of more of these soluble products within the CD11c-depleted fractions.

Each of the proinflammatory mediators measured has been linked experimentally with the severity of renal structural and functional disturbance following IRI and other forms of acute injury.[21–25] Furthermore, a broad range of cytokines and chemokines are elucidated within the injured kidney of which those assayed in this study represent a relatively restricted sample. Nonetheless, we chose to focus subsequent experiments more precisely on defining the
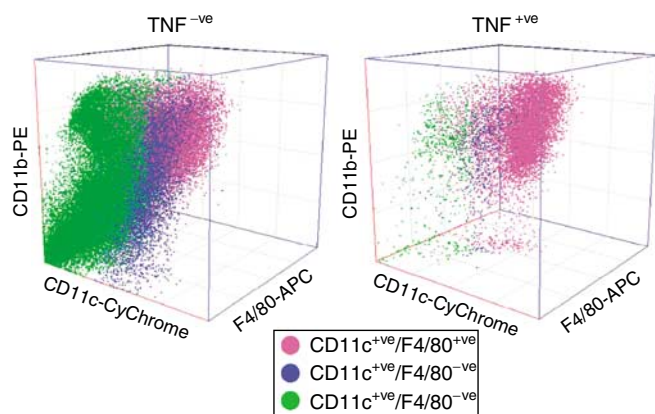
Figure 7 | Predominance of F4/80^{+ve}/CD11b^{+ve} DCs among TNF-expressing cells from ischemic kidneys. A pooled CD45-enriched cell suspension was prepared from three adult mouse kidneys 24 h after 30 min of renal artery clipping. Surface staining with anti-CD11c-CyChrome, anti-CD11b-PE, and anti-F4/80-APC; and intracellular staining with anti-TNF-AF488 was carried out. Three-dimensional dot plots are shown for the surface staining characteristics of TNF^{-ve} (left plot) and TNF^{+ve} cells (right plot) with color coding to indicate CD11c and F4/80 staining status. The TNF^{+ve} cells cluster predominantly as CD11c^{+ve}/F4/80^{+ve}/CD11b^{+ve} population.

Figure 8 | Depletion of intrarenal DCs before onset of IRI results in reduced secretion of TNF by total and CD45^{+ve} kidney cells. (a) Dot plots showing examples of kidney cell suspensions from mice treated 48 h previously with inert (PBS) liposomes or with clodronate-containing liposomes (clodronate) and surface stained for CD45 and CD11c. The percent of total cell suspensions that were CD45^{+ve}/CD11c^{-ve} and CD45^{+ve}/CD11c^{+ve} are indicated for the two samples. (b) Results are shown of ELISA for TNF carried out on culture supernatants from kidney cell fractions of mice pretreated with inert (PBS) liposomes or with clodronate-containing (clodronate) liposomes ($n = 4$ each) then subjected to 30 min of left renal artery clipping. Cells fractions were prepared 24 h following IRI. Left graph: results are shown for equal numbers (10^5 cells/well) of CD45-enriched and CD45-depleted cells from clipped (IRI) and unclipped (Ctrl) kidneys from the two groups. Right graph: results are shown for equal numbers (5×10^5 cells/well) of unfractionated (total) cells and CD45-depleted cells from clipped (IRI) and unclipped (Ctrl) kidneys of the two groups. † = $P < 0.05$ for CD45-enriched vs CD45-depleted (left graph) or total cells vs CD45-depleted (right graph). ‡ = $P < 0.05$ for IRI vs Ctrl kidney for each group. ¶ = $P < 0.05$ for PBS vs equivalent clodronate sample.

contribution of intrarenal DCs and other cell populations to TNF production. This focus stemmed, primarily, from the well-established nonredundant role for TNF in determining the severity of acute renal dysfunction following sepsis, IRI, and other forms of kidney injury.[20,26–28] In animal models of IRI, increased whole-kidney TNF content has been repeatedly demonstrated within 1–4 h of reperfusion and blockade or genetic absence of TNF effector function attenuates subsequent cellular infiltration, epithelial damage, and renal functional impairment.[4,26,28] Intracellular signaling through TNF receptors is associated with upregulation of adhesion molecules and additional proinflammatory mediators as well as with the triggering of apoptosis in renal tubular epithelial cells.[28]

A substantial number of studies have demonstrated the capacity for bone marrow- and monocyte-derived DCs as well as DCs from lymphoid tissues to secrete high levels of TNF and other innate immune mediators following the application of maturation stimuli.[29–31] Despite this, the *in situ* identification of organ-specific DCs as predominant sources of TNF in the early course of tissue injury and immune-mediated diseases has been reported only infrequently.[32] In the case of acute renal IRI, secretion of TNF is conventionally ascribed to infiltrating monocytes, resident or infiltrating macrophages, and tubular epithelial cells.[3,10,33,34] Although there is cumulative evidence that these cell populations represent potential sources of inducible TNF production in the post-IRI kidney, our results in the currently employed unilateral renal artery clip model indicate that the largest population of cells highly positive for intracellular TNF staining at 24 h expressed DC surface markers and exhibited characteristic features of DC maturation including upregulation of MHC II and multiple
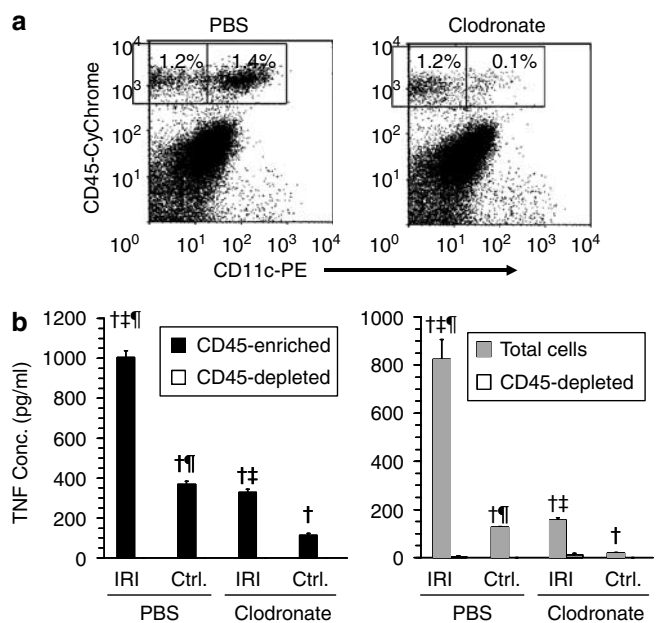
costimulatory ligands. Although infiltration of the postischemic kidney by monocytes, neutrophils, helper, and cytotoxic T cells and, to a lesser extent, F4/80^{-ve} DCs was well demonstrated during these experiments, only monocytes were also observed to comprise a notable proportion (approximately 20%) of the TNF^{+ve} cells. Comparison of TNF^{+ve} monocytes and DCs indicated that the latter were more numerous and expressed higher levels of TNF. Furthermore, predepletion of DCs from the kidney was associated with marked reduction in TNF secretion by CD45^{+ve} kidney cells following IRI. Importantly and in keeping with reported effects of clodronate-containing liposomes on splenic DC populations,[35] this intervention was associated primarily with depletion of resident interstitial DCs from the kidney and did not, in these experiments, result in absence or marked reduction of monocytes (Figure S10), neutrophils, or T cells among the CD45^{+ve} fractions of

ischemic kidneys. It should be noted that Day et al.[34] and Jo et al.[36] have recently reported that clodronate administration results in amelioration of acute renal injury following renal artery clipping in rodent models. In these studies, however, clodronate therapy was clearly also associated with systemic depletion of macrophages and circulating monocytes. Thus, although our results with clodronate-mediated depletion serve as further confirmation that DCs are the predominant local source of TNF following IRI, they cannot be interpreted as indicating that depletion of DCs alone is sufficient to reduce the severity of renal functional impairment. TNF production by CD45$^-$ cell populations (which presumably includes tubular epithelial cells, fibroblasts, endothelial cells, and mesangial cells) was consistently minimal by flow cytometry as well as by magnetic column separation with anti-CD45 microbeads.

Our results highlight an existing ambiguity in the distinction between resident macrophages and DCs in the healthy and injured kidney. Ultrastructural analyses of the renal interstitium indicate that DCs are abundant in the peritubular interstitial space, are morphologically distinct from macrophages, and express high surface levels of MHC II in the resting state.[11–13] In contrast, cells with morphological characteristics of macrophages are sparse and confined, during health, to the periarterial connective tissue, capsule, and pelvic wall.[11,12] Recently, Soos et al.[19] have unequivocally confirmed the extent of the DC network within the renal interstitium of the healthy kidney and have demonstrated the degree to which these cells probe the interstitial microenvironment. This and other studies focused on phenotypic and functional properties of rDCs have confirmed additional expected characteristics including expression of CD11c (a DC-specific marker in the mouse); regulated expression of costimulatory ligands; antigen-uptake and presentation capacity; and migration to T-cell zones of draining lymph nodes following maturational stimuli.[14,15,17,18,37] In keeping with Soos et al.[19] and Kruger et al.,[18] we observe here that a proportion of rDCs express surface or intracellular proteins often considered to represent macrophage markers – F4/80, CD68, and FcγII/III. Despite this apparent phenotypic overlap with resident macrophages, we have shown that these cells migrate out of the injured kidney to draining lymph nodes between 24 and 48 h following an acute injury – a classic DC functional characteristic.[15] The current results also indicate that CD11c^{+ve}/F4/80^{+ve} cells in 24 h ischemic kidneys have higher surface levels of DC maturation markers such as MHC II and costimulatory ligands than those of control kidneys. Although possible explanations for the increased maturation marker levels on intrarenal DCs after IRI include replacement of the original DCs with new, more mature DCs, this is less likely given the fact that this population did not change proportionately within the kidney. Furthermore, we have observed increased surface maturation markers and TNF production by intrarenal DCs as little as 4 h following IRI (X Dong and M Griffin, unpublished observation). Thus, we favor the conclusions

that, in the mouse at least, F4/80^{+ve} or CD68^{+ve} cells in the renal interstitium during health are more likely to represent DCs than macrophages[18,34,38–40] and that these resident intrarenal DCs undergo maturation in situ in the early postischemic time period. Although not within the scope of the current study, it is likely that, at later time points following acute injury, the interstitial space contains a dynamic mixture of persistent resident DCs as well as new populations of DCs and macrophages differentiated from influxing monocytes. Our results do not, therefore, preclude critical roles for infiltrating activated macrophages in the progression of intrarenal inflammation following acute injury and in modulating the extent of eventual tissue repair.[33] Given the divergent immunological roles for DCs and macrophages as well as the potential to individually target them for therapeutic purposes,[33,41] continued efforts at phenotypic and functional distinction between DCs and macrophages in the context of kidney disease models is merited.

The presence of F4/80^{+ve} DCs in the renal interstitium has also been demonstrated by immunostaining of renal tissue sections[18,19,40] and it is interesting to note that, in some studies, this population was most clearly localized to the medulla and juxtamedullary cortex – a region that is more susceptible to severe cellular injury following IRI.[19,40] It is possible, therefore, that exposure of the F4/80^{+ve} DCs to endogenous-activating factors in this region of high cellular injury results in their preferential upregulation of maturation markers and production of TNF. Alternatively, an element of the vulnerability of this region to cellular injury following IRI could be the presence of high levels of DC-produced TNF and other factors. Although it is beyond the scope of this study to determine whether either or both of these relationships exist, additional investigation may clarify the significance of the localization of F4/80^{+ve} DCs within the kidney. It is also of interest to consider which endogenous-activating factors may be directly responsible for stimulating TNF secretion and other IRI-related responses of renal F4/80^{+ve} DCs. Recent progress in understanding innate immune responses to infectious and noninfectious forms of tissue injury have identified a broad range of candidate DC-activating factors released by parenchymal cells exposed to acutely stressful conditions including reactive oxygen species, heat-shock proteins, extracellular matrix components, poly-nucleotides, and other diverse 'danger signals' or 'alar-mins.'[41–45] As tissue-resident DCs express multiple pattern recognition receptors, we would speculate that an array of such endogenous ligands contribute to the DC responses we have observed in the current model. Nonetheless, the role of individual candidate activators and receptors (e.g., toll-like receptors) will be testable in the context of existing mouse strains and reagents.[41,45]

In conclusion, this study provides novel evidence that resident DCs constitute the predominant 'first responders' in the secretion of TNF and other inflammatory mediators that participate in the early pathophysiological events leading to

functional impairment in the acutely injured kidney. Being localized to the peritubular epithelial space and, as we show here, capable of rapid, high-level production of key cytokines and chemokines, rDCs are uniquely positioned to respond to endogenous activators of innate immunity, to instigate secondary responses in renal epithelial and endothelial cells, and to participate in the recruitment of additional circulating cells to the kidney. We propose that further characterization of this cell population in the injured kidney will identify opportunities for manipulating the contributions of innate as well as cognate immunity to acute kidney failure.

MATERIALS AND METHODS
Animals and reagents
Adult C57BL/6 (B6) mice were purchased from The Jackson Laboratory, Bar Harbor, Maine and housed in a specific pathogen-free facility. Tissue culture was carried out in Dulbecco's modified Eagle's medium (DMEM) supplemented with 10% fetal calf serum fetal calf serum (FCS). Detection agents (clone numbers) used in various experiments were anti-CD11c-PE and -biotin (HL3), anti-CD45-biotin (104), anti-Ly6C-FITC (AL-21), anti-Ly6G-FITC (1A8), anti-CD3ε-FITC (2C11), anti-CD80-PE (16-10A1), anti-CD86-PE (GL1), anti-CD54-PE (3E2), anti-CD40-PE (3/23), anti-I-A^b-PE (AF6-120.1), anti-CD8α-PE (53-6.7), anti-CD4-PE (L3T4), anti-CD1d-FITC (1B1), anti-CD11b-PE (M1/70), anti-TNF-APC, - AF488 and purified (MP6-XT22), rat IgG1-APC and -AF488 (R3-34), rat IgG2b-PE and -FITC (a95-1), hamster IgG1-PE (anti-TNP), anti-rat Ig-biotin, streptavidin–cyChrome and -HRP (all from BD Pharmingen, San Jose, CA, USA); anti-F4/80-APC (A3-1), anti-CD169-FITC (3d6.112), anti-CD16/CD32-AF647 (FCR4G8), anti-CD68-AF647 (FA-11), anti-CD204-AF647 (2F8), anti-CD205-AF647 (NLDC-145), rat IgG2a-PE, -FITC and -AF647 (YTH71.3) (all from Serotec Inc., Raleigh, NC, USA); 33D1-PE (from eBioscience, San Diego, CA, USA).

Mouse model of IRI and preparation of kidney cell suspension
Unilateral renal artery clipping was carried out for 30 min in adult mice by pentobarbitol anesthesia as described previously.[15] Kidneys were dissected, cut into 1–2 mm^3 pieces, placed in DMEM containing 1.6 mg/ml collagenase I (Sigma Aldrich, St Louis, MO, USA), and 200 μg/ml DNase I (Roche Applied Science, Indianapolis, IN, USA) for 40 min at 37°C with intermittent agitation, washed, resuspended in DMEM/200 μg/ml DNase I at room temperature for 15 min, and washed twice in DMEM. Following erythrocyte lysis, cells were resuspended in DMEM/10% FCS or FACs buffer (PBS/0.2% bovine serum albumin (BSA)/0.02%NaN$_2$). To ensure that large cellular clumps and noncellular material were not included, kidney cell suspensions to be used for flow cytometry were allowed to settle for 20 min following which the upper two-thirds were removed for use in these assays.

Magnetic column enrichment of CD11c^{+ve} cells, cell culture, and ELISA of culture supernatants
Magnetic bead enrichment and depletion of DCs from kidney cell suspensions were carried out using anti-CD11c-coated microbeads and the miniMACS™ separation system (Miltenyi Biotech Inc., Auburn, CA, USA) according to the manufacturer's instructions. Experiments involving culture of total cells and magnetic column cell fractions were carried out overnight in 96-well round bottom plates following which supernatants were removed and subjected to ELISA for TNF, IL-6, (BD Pharmingen), MCP-1 and RANTES (R&D Systems, Minneapolis, MN, USA). For experiments comparing CD11c-enriched and CD11c-depleted fractions, cells were plated at 10^5 per well with 3–6 wells for each condition. For experiments comparing unsorted and CD11c-depleted fractions, cells were plated at 5 × 10^5 per well with 3–6 wells for each condition.

Immunohistochemistry and immunofluorescence microscopy
Cell suspensions from ischemic and control kidneys were cultured in DMEM/10% FCS containing 1 μg/ml GolgiPlug™ (BD Pharmingen) for 4 h at 37°C then lifted and added to wells of adhesion slides (Erie Scientific, Portsmouth, NH, USA). Immunoperoxidase staining was carried out as described previously[15] using rat anti-TNF or isotype control followed by biotinylated anti-rat antibody, then developed using Vectorstain® Elite ABC solution (Vector Laboratories Inc., Burlingame, CA, USA) followed by diaminobenzidine (DAB) substrate solution. Slides were examined by light microscopy and positively stained cells were enumerated in 10 high-power fields per slide. Immunofluorescence staining was carried out as described previously[15] using rat anti-TNF and hamster anti-CD11c antibodies or isotype controls followed by Alexa Fluor® 488-conjugated anti-rat IgG and Alexa Fluor® 594-conjugated goat-anti hamster IgG. The slides were mounted using VECTASHIELD® mounting medium with 4′,6-diamidino-2-phenylindole (Vector Laboratories) and examined under confocal laser-scanning microscopy (LSM510, Carl Zeiss, Goettingen, Germany).

Flow cytometric analysis
Aliquots of cells were incubated in FACs buffer (PBS/0.2%BSA/0.02%NaN$_2$) at 4°C with combinations of fluorochrome-labeled and/or biotinylated antibodies followed by fluorochrome-labeled strep-tavidin. Intracellular staining of kidney cells was carried out using the Cytofix/Cytoperm™ kit (BD Pharmingen). For experiments involving intracellular staining of TNF, suspensions were cultured for 8 h in DMEM/10% FCS containing 1 μl/ml of GolgiPlug™ reagent (BD Pharmingen) before staining. Samples were analyzed using a fluorescence-activated cell sorter (FACS) Calibur™ flow cytometer and Cellquest™ software (BD Pharmingen).

Clordonate liposome-mediated depletion of intrarenal DCs
Clodronate (dichloromethylene bisphosphonate, Sigma Aldrich) liposomes were prepared by the method of Van Rooijen et al.[46] Briefly, phosphatidylcholine (86 mg of egg lecithin in 4.3 ml chloroform) and cholesterol (8 mg in 10 ml chloroform) were evaporated by rotation under reduced pressure. Clodronate (2.5 g in 10 ml of H$_2$O) was added to disperse the lipid gently. The lipid suspension was placed under N$_2$ for 2 hours, sonicated, washed, and resuspended in 4 ml of sterile PBS. Inert liposomes were prepared by the same protocol with PBS alone. Adult mice were injected intravenously with 200 μl of clodronate- or PBS-liposomes on 2 consecutive days. Mice were subjected to unilateral renal artery clipping 48 h after the second injection.

Statistical analysis
Numerical results for individual experimental groups were expressed as mean ± s.d. and were compared using paired (for left vs right kidney experiments) or unpaired (for all other comparisons) two-sided Student's t-test with significance assigned to $P < 0.05$. Experiments were carried out between three and six times to ensure reproducibility.

SUPPLEMENTARY MATERIAL

Figure S9. Flow cytometric histograms are shown for staining of CD45 + ve/CD11c + ve cells from suspensions of healthy adult mouse kidneys.

Figure S10. Results of staining and quantification of DCs and monocytes are shown for ischemic and control kidneys of mice pretreated with inert (PBS) liposomes or clodronate-containing liposomes.

REFERENCES

1. Bonventre JV, Weinberg JM. Recent advances in the pathophysiology of ischemic acute renal failure. *J Am Soc Nephrol* 2003; **14**: 2199–2210.
2. Boros P, Bromberg JS. New cellular and molecular immune pathways in ischemia/reperfusion injury. *Am J Transplant* 2006; **6**: 652–658.
3. Friedewald JJ, Rabb H. Inflammatory cells in ischemic acute renal failure. *Kidney Int* 2004; **66**: 486–491.
4. Takada M, Nadeau KC, Shaw GD et al. The cytokine-adhesion molecule cascade in ischemia/reperfusion injury of the rat kidney. Inhibition by a soluble P-selectin ligand. *J Clin Invest* 1997; **99**: 2682–2690.
5. Crisman JM, Richards LL, Valach DP et al. Chemokine expression in the obstructed kidney. *Exp Nephrol* 2001; **9**: 241–248.
6. Lemay S, Rabb H, Postler G et al. Prominent and sustained up-regulation of gp130-signaling cytokines and the chemokine MIP-2 in murine renal ischemia–reperfusion injury. *Transplantation* 2000; **69**: 959–963.
7. Maier S, Emmanuilidis K, Entleutner M et al. Massive chemokine transcription in acute renal failure due to polymicrobial sepsis. *Shock* 2000; **14**: 187–192.
8. Day Y-J, Huang L, McDuffie MJ et al. Renal protection from ischemia mediated by A2A adenosine receptors on bone marrow-derived cells. *J Clin Invest* 2003; **112**: 883–891.
9. Burton CJ, Combe C, Walls J et al. Secretion of chemokines and cytokines by human tubular epithelial cells in response to proteins. *Nephrol Dial Transplant* 1999; **14**: 2628–2633.
10. Jevnikar AM, Brennan DC, Singer GG et al. Stimulated kidney tubular epithelial cells express membrane associated and secreted TNF alpha. *Kidney Int* 1991; **40**: 203–211.
11. Lemley KV, Kriz W. Anatomy of the renal interstitium. *Kidney Int* 1991; **39**: 370–381.
12. Kaissling B, Le Hir M. Characterization and distribution of interstitial cell types in the renal cortex of rats. *Kidney Int* 1994; **45**: 709–720.
13. Steptoe RJ, Patel RK, Subbotin VM et al. Comparative analysis of dendritic cell density and total number in commonly transplanted organs: morphometric estimation in normal mice. *Transplant Immunol* 2000; **8**: 49–56.
14. Larsen CP, Ritchie SC, Hendrix R et al. Regulation of immunostimulatory function and costimulatory molecule (B7-1 and B7-2) expression on murine dendritic cells. *J Immunol* 1994; **152**: 5208–5219.
15. Dong X, Swaminathan S, Bachman LA et al. Antigen presentation by dendritic cells in renal lymph nodes is linked to systemic and local injury to the kidney. *Kidney Int* 2005; **68**: 1096–1108.
16. Austyn JM, Hankins DF, Larsen CP et al. Isolation and characterization of dendritic cells from mouse heart and kidney. *J Immunol* 1994; **152**: 2401–2410.
17. Roake JA, Rao AS, Morris PJ et al. Dendritic cell loss from nonlymphoid tissues after systemic administration of lipopolysaccharide, tumor necrosis factor, and interleukin 1. *J Exp Med* 1995; **181**: 2237–2247.
18. Kruger T, Benke D, Eitner F et al. Identification and functional characterization of dendritic cells in the healthy murine kidney and in experimental glomerulonephritis. *J Am Soc Nephrol* 2004; **15**: 613–621.
19. Soos TJ, Sims TN, Barisoni L et al. CX3CR1+ interstitial dendritic cells form a contiguous network throughout the entire kidney. *Kidney Int* 2006; **70**: 591–596.
20. Ramesh G, Reeves WB. TNFα mediates chemokine and cytokine expression and renal injury in cisplatin nephrotoxicity. *J Clin Invest* 2002; **110**: 835–842.
21. Rice JC, Spence JS, Yetman DL et al. Monocyte chemoattractant protein-1 expression correlates with monocyte infiltration in the post-ischemic kidney. *Renal* 2002; **24**: 703–723.
22. Viedt C, Orth SR. Monocyte chemoattractant protein-1 (MCP-1) in the kidney: does it more than simply attract monocytes? *Nephrol Dial Transplant* 2002; **17**: 2043–2047.
23. Song E, Zou H, Yao Y et al. Early application of Met-RANTES ameliorates chronic allograft nephropathy. *Kidney Int* 2002; **61**: 676–685.
24. Patel NS, Chatterjee PK, Di Paola R et al. Endogenous interleukin-6 enhances the renal injury, dysfunction, and inflammation caused by ischemia/reperfusion. *J Pharm Exp Ther* 2005; **312**: 1170–1178.
25. Holdsworth SR, Kitching AR, Tipping PG. Chemokines as therapeutic targets in renal disease. *Curr Opin Nephrol Hypertens* 2000; **9**: 505–511.
26. Donnahoo KK, Meng X, Ayala A et al. Early kidney TNF-alpha expression mediates neutrophil infiltration and injury after renal ischemia–reperfusion. *Am J Physiol Regul Integr Comp Physiol* 1999; **277**: R922–R929.
27. Misseri R, Meldrum DR, Dinarello CA et al. TNF-alpha mediates obstruction-induced renal tubular cell apoptosis and proapoptotic signaling. *Am J Physiol – Renal Physiol* 2005; **288**: F406–F411.
28. Donnahoo KK, Shames BD, Harken AH et al. Review article: the role of tumor necrosis factor in renal ischemia–reperfusion injury. *J Urol* 1999; **162**: 196–203.
29. Fischer FR, Luo Y, Luo M et al. RANTES-induced chemokine cascade in dendritic cells. *J Immunol* 2001; **167**: 1637–1643.
30. Efron P, Moldawer LL. Sepsis and the dendritic cell. *Shock* 2003; **20**: 386–401.
31. Voisine C, Hubert FX, Trinite B et al. Two phenotypically distinct subsets of spleen dendritic cells in rats exhibit different cytokine production and T cell stimulatory activity. *J Immunol* 2002; **169**: 2284–2291.
32. Dahlen E, Dawe K, Ohlsson L et al. Dendritic cells and macrophages are the first and major producers of TNFα in pancreatic islets in the nonobese diabetic mouse. *J Immunol* 1998; **160**: 3585–3593.
33. Kluth DC, Erwig LP, Rees AJ. Multiple facets of macrophages in renal injury. *Kidney Int* 2004; **66**: 542–557.
34. Day YJ, Huang L, Ye H et al. Renal ischemia–reperfusion injury and adenosine 2A receptor-mediated tissue protection: role of macrophages. *Am J Physiol – Renal Physiol* 2005; **288**: F722–F731.
35. Leenen PJ, Radosevic K, Voerman JS et al. Heterogeneity of mouse spleen dendritic cells: in vivo phagocytic activity, expression of macrophage markers, and subpopulation turnover. *J Immunol* 1998; **160**: 2166–2173.
36. Jo S-K, Sung S-A, Cho W-Y et al. Macrophages contribute to the initiation of ischaemic acute renal failure in rats. *Nephrol Dial Transplant* 2006; **21**: 1231–1239.
37. Kurts C. Dendritic cells: Not just another cell type but a complex immune sentinel network. *Kidney Int* 2006; **70**: 412–414.
38. Lenda DM, Kikawada E, Stanley ER et al. Reduced macrophage recruitment, proliferation, and activation in colony-stimulating factor-1-deficient mice results in decreased tubular apoptosis during renal inflammation. *J Immunol* 2003; **170**: 3254–3262.
39. Cailhier JF, Partolina M, Vuthoori S et al. Conditional macrophage ablation demonstrates that resident macrophages initiate acute peritoneal inflammation. *J Immunol* 2005; **174**: 2336–2342.
40. Hume DA, Gordon S. Mononuclear phagocyte system of the mouse defined by immunohistochemical localization of antigen F4/80. Identification of resident macrophages in renal medullary and cortical interstitium and the juxtaglomerular complex. *J Exp Med* 1983; **157**: 1704–1709.
41. Anders HJ, Banas B, Schlondorff D. Signaling danger: toll-like receptors and their potential roles in kidney disease. *J Am Soc Nephrol* 2004; **15**: 854–867.
42. Oppenheim JJ, Yang D. Alarmins: chemotactic activators of immune responses. *Curr Opin Immunol* 2005; **17**: 359–365.
43. Johnson GB, Brunn GJ, Kodaira Y et al. Receptor-mediated monitoring of tissue well-being via detection of soluble heparan sulfate by Toll-like receptor 4. *J Immunol* 2002; **168**: 5233–5239.
44. Beg AA. Endogenous ligands of Toll-like receptors: implications for regulating inflammatory and immune responses. *Trend Immunol* 2002; **23**: 509–512.
45. Leemans JC, Stokman G, Claessen N et al. Renal-associated TLR2 mediates ischemia/reperfusion injury in the kidney. *J Clin Invest* 2005; **115**: 2894–2903.
46. Van Rooijen N, Sanders A. Liposome mediated depletion of macrophages: mechanism of action, preparation of liposomes and applications. *J Immunol Methods* 1994; **174**: 83–93.